HHS Public Access

Author manuscript

Magn Reson Med. Author manuscript; available in PMC 2023 November 01.

Published in final edited form as:

Magn Reson Med. 2022 November ; 88(5): 2233–2241. doi:10.1002/mrm.29353.

Quantitative cerebrovascular reactivity MRI in mice using acetazolamide challenge

Zhiliang Wei[1,2,*], **Yuguo Li**[1,2], **Xirui Hou**[3], **Zheng Han**[1,2], **Jiadi Xu**[1,2], **Michael T. McMahon**[1,2], **Wenzhen Duan**[4,5], **Guanshu Liu**[1,2], **Hanzhang Lu**[1,2,3]

[1]Russell H. Morgan Department of Radiology and Radiological Science, Johns Hopkins University School of Medicine, Baltimore, Maryland, USA.

[2]F. M. Kirby Research Center for Functional Brain Imaging, Kennedy Krieger Research Institute, Baltimore, Maryland, USA.

[3]Department of Biomedical Engineering, Johns Hopkins University School of Medicine, Baltimore, Maryland, USA.

[4]Department of Psychiatry and Behavioral Sciences, Johns Hopkins University School of medicine, Baltimore, Maryland, USA.

[5]The Solomon H. Snyder Department of Neuroscience, Johns Hopkins University School of medicine, Baltimore, Maryland, USA.

Abstract

Purpose: To develop a quantitative MRI method to estimate cerebrovascular reactivity (CVR) in mice.

Methods: We described an MRI procedure to measure cerebral vasodilatory response to acetazolamide (ACZ), a vasoactive agent previously used in human clinical imaging. Vascular response was determined by cerebral blood flow (CBF) measured with phase-contrast or pseudo-continuous arterial-spin-labeling (pCASL) MRI. Vasodilatory input intensity was determined by plasma ACZ level using high-performance liquid chromatography (HPLC). We verified the source of the CVR MRI signal by comparing ACZ injection to phosphate-buffered saline (PBS) injection and non-injection experiments. Dose dependence and feasibility of regional CVR measurement were also investigated.

Results: CBF revealed an exponential increase upon intravenous ACZ injection, with a time constant of 1.62 minutes. In contrast, PBS- or non-injection exhibited a slow linear CBF increase, consistent with a gradual accumulation of anesthetic agent, isoflurane, used in this study. When comparing different ACZ doses, injections of 30, 60, 120, and 180 mg/kg yielded a linear increase in plasma ACZ concentration ($P<0.0001$). On the other hand, CBF changes under these doses were not different from each other ($P=0.50$). The pCASL MRI with multiple post-labeling delays (PLDs) revealed similar vascular responses at different PLD values. There was a regional difference in CVR ($P=0.005$) with isocortex ($0.81\pm0.17\%/[\mu g/ml]$) showing higher CVR than

[*]Corresponding author: Zhiliang Wei, Ph.D., The Russell H. Morgan Department of Radiology and Radiological Science, Johns Hopkins University School of Medicine, 600 N. Wolfe Street, Park 326, Baltimore, MD 21287, zhiliang.wei@jhu.edu, Phone: 443-453-2581, Fax: 410-614-1977.

deep-brain regions. Mice receiving multiple ACZ injections lived for a minimum of 6 months after the study without noticeable aberrant behavior or appearance.

Conclusion: We demonstrated the proof-of-principle of a new quantitative CVR mapping technique in mice.

Keywords

acetazolamide; cerebral blood flow; cerebrovascular reactivity; phase contrast; arterial spin labeling; mouse; MRI

INTRODUCTION

Cerebrovascular reactivity (CVR) denotes the brain's vasodilatory capacity and provides a quantitative evaluation of vascular reserve.[1] In humans, CVR has been measured with MRI by applying vasoactive challenges such as carbon dioxide (CO_2) inhalation,[2–4] breath holding,[5,6] or breath modulation.[7] Measurements of both input (e.g. end-tidal CO_2, $EtCO_2$) and output (e.g. blood-oxygenation-level-dependent (BOLD) signal or cerebral blood flow (CBF) signal) can then yield an CVR estimation.[2] Due to its excellent sensitivity to microvascular function, CVR MRI has received surging interests in recent years and has been applied to studies of Alzheimer's disease,[4,8] vascular dementia,[9,10] multiple sclerosis,[11,12] brain tumor,[13,14] stroke,[15] Moyamoya disease,[16] and sickle cell disease.[17]

While these human investigations are important in demonstrating the utility of CVR MRI in clinical settings, animal model studies are invaluable for validating and characterizing new biomarkers, initial testing of new drugs, and longitudinal studies to determine disease progression. However, there is a scarcity of techniques or reports of quantitative CVR mapping in mice. In particular, the widely used CO_2-based method has not been successfully used in mice due to their low breathing volume and high breathing rate. The sampled inhaled/exhaled gas will experience severe mixing along the sampling tube before detected, thus prohibiting the accurate $EtCO_2$ determination. Without the knowledge of $EtCO_2$, quantitative CVR (i.e. per mmHg value) cannot be determined.

In this study, we took a different approach by using a pharmacological stimulus, acetazolamide (ACZ),[18–20] which has been shown capable of inducing vasodilatory responses. ACZ is a carbonic anhydrase inhibitor and has been commonly used as diuretic medication in the treatment of glaucoma,[21] epilepsy,[22] and high-altitude sickness.[23] It has also been used as a vasoactive agent in diagnostic imaging in stenotic diseases such as Moyamoya disease.[24,25] Thus the development of an ACZ-based CVR technique in mice will have direct human relevance. In this study, plasma level of ACZ (i.e., $[ACZ]_{plasma}$) was determined with a high-performance liquid chromatography (HPLC)[26] to provide a quantitative measure of stimulus strength. The vascular response was quantified by MRI measurement of CBF with phase-contrast (PC)[27] or pseudo-continuous arterial spin labeling (pCASL)[28] MRI. To confirm that the observed vascular responses is attributed to ACZ injection rather than other factors, e.g. time-dependent changes in anesthesia level or dilution effect of fluid injection, we compared the result of ACZ injection with those of phosphate-

buffered saline (PBS) injection and no injection. Dose dependence of vascular responses on ACZ was also investigated.

METHODS

General procedure of CVR MRI using ACZ challenge

Figure 1 shows a schematic diagram of CVR MRI using ACZ challenge. A CVR experiment consisted of animal preparation, MRI scan with ACZ injection, blood sample collection and processing, and HPLC analyses. For animal preparation, a needle (30G, 0.3mm×13mm, Precision-Glide needles, Becton-Dickinson & Co, USA) was inserted into the tail vein of the mouse and was connected to a syringe (1 ml TB syringe, Becton-Dickinson & Co, USA) containing the ACZ solution (X-GEN Pharmaceuticals Inc., New York, USA) with an extension polyethylene tubing (I.D. 0.28mm, Becton-Dickinson & Co, USA). After the preparation, mouse was transported to the MRI scanner for pre-injection CBF scans. Injection volume was 6 μL per gram body weight and injection was administered with an injection pump (PHD 2000, Harvard apparatus, Massachusetts, USA) at an injection rate of 150 μL/min. CBF MRI protocols were utilized at pre- and post-injection to measure perfusion changes (Figure 1A). Immediately following the MRI session, a few drops of blood (total volume <90 μL) were collected into a microtainer (600 μL, lithium heparin coated, Becton-Dickinson & Co, USA) using the submandibular bleeding method[29] outside the scanner (Figure 1A). $[ACZ]_{plasma}$ was then measured by HPLC (Bio-Rad, Melbourne, Australia) (see Supporting Information for more details). CVR was then calculated as the percentage change in CBF divided by $[ACZ]_{plasma}$ (Figure 1A):

$$CVR = \frac{100(CBF_{post} - CBF_{pre})/CBF_{pre}}{[ACZ]_{plasma}}, \quad [1]$$

where CBF_{pre} and CBF_{post} denotes CBF measured at pre-injection and post-injection, respectively; the unit of CVR is %/[μg/ml].

MRI experiments

All MRI experiments were performed on an 11.7T Bruker Biospec system (Bruker, Ettlingen, Germany) with a horizontal bore as well as an actively shielded pulse field gradient (maximum intensity of 0.74 T/m). The institutional animal care and use committee approved the experimental protocol. Nine C57BL/6 mice (age: 28–46 weeks; body weight: 23–32g) was used in present study. All mice had free access to food and water and were housed in a quiet environment with a 12-h day/night cycle. Isoflurane was used as anesthesia as previously described (1.0–1.2% for maintenance).[30] Images were acquired using a 72-mm quadrature volume resonator as transmitter, and a four-element (2×2) phased-array coil as receiver.

A total of 38 MRI sessions were conducted, including four sub-studies focusing on vascular response characterization (Study 1), dose dependence (Study 2), and regional CVR mapping (Study 3&4), respectively. The same cohort of 5 female mice were tested in Study 1and Study 2; another cohort of 4 mice (2 female and 2 male) were used in Study 3; 4 mice from Study 1&2 were used in Study 4.

Study 1: Characterization of vascular response following ACZ injection.—To demonstrate the causal relationship between ACZ injection and CBF changes, each mouse underwent three experimental sessions on different days (≥72 hours apart): ACZ injection (dose at 30 mg/kg), PBS injection, and no injection. PBS was injected at the same volume as ACZ solution to investigate the potential dilution effects (e.g. anesthetic dilution or hemodilution effect[31]) induced by transient increase in total plasma volume. The session without injection was conducted to evaluate the potential change in anesthesia level during the experiment.

To maximize signal-to-noise ratio and temporal resolution, phase-contrast (PC) MRI was applied on the left internal carotid artery (LICA). Imaging procedures for the mouse PC MRI have been optimized and described previously.[32] Key parameters of PC MRI were: TR/TE=15/3.2 ms, encoding velocity = 20 cm/s, and scan duration = 2.4 min (see Supporting Information for more details).

Study 2: Dose dependence of CBF response to ACZ.—A total of four different doses (30, 60, 120, and 180 mg/kg) were studied in each mouse. Different doses for a same mouse were tested on different days (at least 72 hours apart). The 30 mg/kg dose used the same data as those in Study 1. Thus, each mouse received three additional MRI sessions in this sub-study (60, 120, and 180 mg/kg). For different doses, the concentrations of ACZ solutions were varied so that the injection volumes were kept the same. The MRI protocols in Study 1 were used in Study 2, and the timeline was shown in Figure 1C. The order of receiving the additional doses was randomized and counterbalanced across animals, following a previously reported scheme.[33]

Study 3: Regional vascular response with multiple PLDs.—This study focused on the feasibility of regional vascular response mapping (HPLC not used). To investigate the dependence of pCASL-based vascular response on post-labeling delay (PLD) values, 6 difference PLDs (50, 150, 300, 450, 600 and 800 ms) were used in this study. Note that the data were sampled more densely in the shorter PLDs than longer ones, because the signal in the kinetic curve changes more rapidly in early times. The pCASL MRI was first performed to map pre-injection perfusion and repeated after a 10 min awaiting time, during which ACZ injection was administered (Figure 1D).

A two-scan pCASL scheme[33–35] was utilized. Key parameters for pCASL scan were (see Supporting Information for more details): TR/TE = 3000/11.8 ms, labeling-pulse width = 0.5 ms, inter-labeling-pulse delay = 1.0 ms, and scan duration = 2.0 min with a two-segment spin-echo echo-planar-imaging acquisition. Scan duration of pCASL at each PLD was 2 min (12 min for 6 PLD, Figure 1D).

Study 4: Regional CVR mapping with single PLD.—After investigating the potential dependence of regional vascular response on PLD values, single-PLD pCASL was implemented along with HPLC to quantify CVR in different brain regions. Experimental parameters and setting were identical with Study 3 except for: PLD = 300 ms and scan time = 5.0 min (more averages than Study 3).

Upon completing all MRI sessions for each mouse, mice receiving multiple doses were kept in the animal facility for ≥6 months before euthanization to allow observations of any long-term side effects induced by ACZ injections and associated MRI experiments.

Data processing

All processing was conducted using custom-written MATLAB (MathWorks, Natick, MA) scripts. PC and pCASL MRI data were processed according to our previous reports.[32,33] CBF weighted images, i.e. CBF_{index} calculated as the difference image of pCASL divided by magnetization at equilibrium, before and after the injection were co-registered and normalized to a mouse brain template (http://www.bmap.ucla.edu/portfolio/atlases/MSA).[36]

Statistical analyses

One-way ANOVA was performed to compare CBF changes among different injection regimens in Study 1, different doses in Study 2, different PLDs in Study 3, and different regions in Study 4.

Linear mixed-effect (LME) model was also employed in Study 1 and Study 2 to examine the time-dependence of CBF changes and the time-by-group interaction effects. Linear regression was used to study the relationship between nominal injection doses and $[ACZ]_{plasma}$. A P value of 0.05 or less was considered as statistically significant.

RESULTS

Study 1

Figure 2A shows CBF responses to the ACZ injection (injection started at 0 min), in comparison with PBS injection and no fluid injection. There was an exponential increase in CBF following ACZ injection ($y = 39.7\%[1 - e^{-x/1.62}]$), which gradually reached a plateau. In contrast, PBS and no injection exhibited slow linear increases with time. There was a significant time-by-injection regimen interaction effect (P<0.0001), suggesting a difference in CBF responses among injection regimens. It was observed that, during 10–20 min post-injection, the CBF response was 99.8% of the steady-state amplitude (last 10 min of experiment). Therefore, 10 min was considered as an approximate steady-state time point and used in later studies.

Averaged CBF changes during 10–20 min post-injection of different groups were summarized in Figure 2B. ANOVA revealed a significant difference among the three groups (P<0.0001). Post-hoc Tukey's honest test revealed a significant $\Delta CBF/CBF_{pre}$ difference between ACZ- and PBS-injection (P=0.0004), and between ACZ- and no-injection (P=0.0002). There was not a difference between PBS- and no-injection (P=0.89).

The no-injection data revealed a time-dependent increase in CBF (LME: P<0.0001), suggesting a drift in the physiological state of mouse without injection. However, there was not a group effect (P=0.23) nor a time-by-group interaction effect (P=0.29) between PBS injection and no-injection, suggesting an insignificant dilution effect.

Study 2

Figure 3A shows HPLC chromatograms of blood samples from a representative mouse following different injections. Referenced to the signal of a standard ACZ solution with known concentration, $[ACZ]_{plasma}$ was calculated and summarized in Figure 3B. A linear relationship between injection dose and $[ACZ]_{plasma}$ was observed ($[ACZ]_{plasma} = 1.04 dose$, $R^2 = 0.76$, $P < 0.0001$). Dynamic curves of CBF changes at different doses largely overlapped with each other (Figure 3C). Quantitative analyses using data acquired during 10–20 min post-injection revealed insignificant difference in CBF changes (Figure 3D, P=0.50). LME analysis with dose as a fixed term and mouse as a random term showed similar results (insignificant dose effect, P=0.16). These data suggested that further increasing dose >30 mg/kg did not provide additional benefit to the detection of vascular response. The dose of 30 mg/kg was therefore used in later studies.

Study 3

Figure 4A displays ASL CBF-weighted images (see Supporting Information for more results) at different PLD times for both pre- and post-injection conditions. Quantitative results of whole-brain CBF_{index} signals are plotted in Figure 4B and CBF_{index} signal decreases monotonically with PLD. This is consistent with simulations with kinetic model and is attributed to a short BAT in mice (Supporting Information Figure S3A). Comparing pre- and post-injection in Figure 4B, the CBF_{index} signal increased consistently across all PLD values. ANOVA test revealed that $\Delta CBF/CBF_{pre}$ was not dependent on PLD (Figure 4C, P=0.94).

Study 4

Figures 5A shows the multi-slice CBF-weighted images for pre- and post-injection conditions. Consistent with Study 3, CBF increases across the whole brain. Figure 5B presents ROIs corresponding to different brain regions overlaid on the averaged pCASL control images. As can be seen in Figure 5C, there was a significant difference in CVR values across brain regions (P=0.005). In general, isocortex (0.81±0.17%/[μg/ml]) was associated with a higher CVR in comparison with deep brain regions (e.g., 0.22±0.03%/[μg/ml] for olfactory area or 0.15±0.03%/[μg/ml] for hypothalamus).

Finally, mice receiving multiple injection doses did not show noticeable aberrant behaviors or appearance over a minimum of 6 months after the final MRI scan, supporting the safety of repeated ACZ injections and associated MRI experiments.

DISCUSSION

We proposed a CVR MRI method in mice using the ACZ challenge. We demonstrated the sensitivity of MRI measurements to the vasodilatory effect of ACZ. Our method provided quantitative CVR values in the unit of %/[μg/ml], thus is suitable for comparison across animals or longitudinal studies of same animals. We further showed that the proposed measurement, despite requiring injection of vasoactive agent, is safe for animals and can be repeated multiple times. We also demonstrated that both global and regional CVR assessments are feasible with the proposed procedures.

Mouse has a much smaller tidal volume and faster breathing rate than human, which precludes accurate recording of CO_2 trace, due to undesired gas mixing. As a result, previous reports of perfusion changes in response to hypercapnia did not accounted for $EtCO_2$, and only provide an index of relative CVR.[37–42] Mechanical ventilation[43] has also been be used in hypercapnia studies of mice, but the CO_2 measurement remained difficult with an added risk of lung injuries.[44] Transcutaneous blood gas monitoring constituted an interesting tool for the quantitative mouse CVR estimation,[45] but its effectiveness was limited to large animal number and tightly controlled condition.[46]

Our results suggested that the CVR data were not strongly dependent on PLD. Theoretical analyses with kinetic modeling also revealed similar conclusions (Supporting Information). The negligible dependence of mouse CVR on PLD primarily originates from its relative measure and short BAT in mice. Following the same principle, we expect that CBF-based CVR measurement in humans will also have minimal dependence on PLD, provided that the PLD is similar or longer than tissue BAT to avoid large vessel contaminations.

The present study presents a different approach for CVR assessment by tail-vein injection of ACZ as a physiological challenge. The major advantage of this approach is the feasibility of determining blood/plasma ACZ concentration with biochemical methods such as HPLC. Clinically, ACZ has been widely used for both treatment and diagnostic purposes. The safety profile of ACZ has been well studied and proven after many years' clinical applications.[47] Our study also prove that ACZ could be repeatedly used for a few times on the same mice on different days without noticeable long-term harms to the mice. On the other hand, although hypercapnia challenge is a popular method in human CVR studies, ACZ-based CVR can serve as a helpful alternative for those suffering from discomfort under hypercapnia.[7] Importantly, ACZ-based CVR has been used clinically to evaluate vascular conditions such as Moyamoya disease, although the plasma concentration of ACZ has not been accounted for.[24] Therefore, the combination of MRI and HPLC may open new avenues of human physiology studies where the intensity of pharmaceutical challenge can be quantified.

A previous report studied the effects of several different anesthetic regimens on CVR estimations.[45] The present work further demonstrated that, for a given anesthesia regimen, time-dependent alterations in anesthesia depth needs to be considered in CVR experiments. Due to the slow process of anesthetic accumulation, the time gap from pre-injection measures to post-injection measures needs to be minimized.

We performed a subtraction between the dynamic curve of ACZ-injection and that of PBS-injection in Study 1 to gain some insight into the ACZ clearance (Figure S4 in Supporting Information). From the difference curve, a gradual decrease trend can be seen from 20 min post-injection and onwards. Fitting the data to LME model, there was a significant decrease ($P<0.0001$) from 20 min post-injection at the rate of −0.4% per min. One can then estimate that the half-life of ACZ in mice (in terms of its effects on CBF) is approximately 55 min. As a reference, a human study reported a half-life of plasma ACZ at 4–6 hours.[48]

We studied the dose range of 30–180 mg/kg and found that animals were well tolerated to even the highest dose of 180 mg/kg, which corresponded to a human equivalent dose[49] of

about 14.6 mg/kg (similar to the human single clinical dose of 1 g for an adult[50]). We also found that higher ACZ doses (>30 mg/kg) did not introduce higher effect in CBF changes. This is possibly because ACZ at 30 mg/kg has already fully relaxed the smooth muscle in the vessel[51], thus the CBF has reached its plateau value. Therefore, 30 mg/kg was used after the dose-dependence study. Future study focusing on vascular responses to <30 mg/kg ACZ injections is needed to refine the optimal dose for CVR measurement.

Regional CBF differences are a common and reproducible finding in both human[52,53] and rodent animals[35,40,54,55]. In the present study, CVR variations across brain regions were also observed. As CVR denotes the vessels' dilatory reserve, it is plausible that these regional differences are associated with vessel density. A fluorescent microscopy study revealed heterogeneous vessel density in both rat and mouse brain.[56] The regional difference in vessel density was reproduced by other studies utilizing histology methods.[57,58]

Results in the current study should be interpreted with limitations. First, the present report should be considered as a proof-of-principle study to demonstrate the initial feasibility of the proposed method. The normative values (ranges) of CVR still need to be established in future studies after the impact of anesthetic types and doses on the measured CVR is better understood. Second, the proposed CVR method requires some expertise and equipment in addition to MRI, such as tail-vein preparation and injection, blood sampling, and HPLC measurement. Thirdly, the pCASL image quality and SNR need to be further improved in order to provide a voxel-by-voxel map of CVR. As a matter of fact, the same issue exists in human CVR studies. Finally, a future study is required to evaluate the accuracy and reproducibility of the ACZ-based CVR measurement. As a proof-of-principle demonstration, we took advantage of availability of multiple dynamics in Study 1. The time window of 10–20 min post-injection was divided into two halves, namely 10–15 min and 15–20 min. The corresponding intra-session coefficient of variation was found to be 7.4±3.0%.

CONCLUSIONS

We established a quantitative CVR MRI method in mice using ACZ challenge. We provided evidence of feasibility, safety, temporal characteristics, spatial resolution, and dose-dependence of this method. Upon future optimization and validation, this new CVR technique may open several avenues of preclinical research on cerebrovascular diseases and their treatments in different animal models.

Supplementary Material

Refer to Web version on PubMed Central for supplementary material.

Grant Sponsors:

NIH R21 NS119960, NIH R21 AG058413, NIH R01 NS106702, NIH R01 NS106711, NIH R01 AG064792, NIH U01 NS100588, and NIH RF1 AG071515.

REFERENCE

1. Fisher JA, Venkatraghavan L, Mikulis DJ. Magnetic resonance imaging-based cerebrovascular reactivity and hemodynamic reserve. Stroke 2018; 49(8): 2011–2018. [PubMed: 29986929]
2. Liu P, De Vis JB, Lu H. Cerebrovascular reactivity (CVR) MRI with CO2 challenge: A technical review. Neuroimage 2019; 187: 104–115. [PubMed: 29574034]
3. Sobczyk O, Crawley AP, Poublanc J et al. Identifying significant changes in cerebrovascular reactivity to carbon dioxide. AJNR Am J Neuroradiol 2016; 37(5): 818–824. [PubMed: 26846924]
4. Sur S, Lin Z, Li Y et al. Association of cerebrovascular reactivity and Alzheimer pathologic markers with cognitive performance. Neurology 2020; 95(8): e962–e972. [PubMed: 32661101]
5. Chan ST, Evans KC, Song TY et al. Cerebrovascular reactivity assessment with O2-CO2 exchange ratio under brief breath hold challenge. PLoS One 2020; 15(3): e0225915. [PubMed: 32208415]
6. Cohen AD, Wang Y. Improving the assessment of breath-holding induced cerebral vascular reactivity using a multiband multi-echo ASL/BOLD sequence. Sci Rep 2019; 9(1): 5079. [PubMed: 30911056]
7. Liu P, Xu C, Lin Z et al. Cerebrovascular reactivity mapping using intermittent breath modulation. Neuroimage 2020; 215: 116787. [PubMed: 32278094]
8. Silvestrini M, Pasqualetti P, Baruffaldi R et al. Cerebrovascular reactivity and cognitive decline in patients with Alzheimer disease. Stroke 2006; 37(4): 1010–1015. [PubMed: 16497984]
9. Gao YZ, Zhang JJ, Liu H et al. Regional cerebral blood flow and cerebrovascular reactivity in Alzheimer's disease and vascular dementia assessed by arterial spinlabeling magnetic resonance imaging. Curr Neurovasc Res 2013; 10(1): 49–53. [PubMed: 23151075]
10. Vicenzini E, Ricciardi MC, Altieri M et al. Cerebrovascular reactivity in degenerative and vascular dementia: a transcranial Doppler study. Eur Neurol 2007; 58(2): 84–89. [PubMed: 17565221]
11. Marshall O, Lu H, Brisset JC et al. Impaired cerebrovascular reactivity in multiple sclerosis. JAMA Neurol 2014; 71(10): 1275–1281. [PubMed: 25133874]
12. Uzuner N, Ozkan S, Cinar N. Cerebrovascular reactivity in multiple sclerosis patients. Mult Scler 2007; 13(6): 737–741. [PubMed: 17613601]
13. Zaca D, Hua J, Pillai JJ. Cerebrovascular reactivity mapping for brain tumor presurgical planning. World J Clin Oncol 2011; 2(7): 289–298. [PubMed: 21773079]
14. Pillai JJ, Mikulis DJ. Cerebrovascular reactivity mapping: an evolving standard for clinical functional imaging. AJNR Am J Neuroradiol 2015; 36(1): 7–13. [PubMed: 24788129]
15. Reinhard M, Schwarzer G, Briel M et al. Cerebrovascular reactivity predicts stroke in high-grade carotid artery disease. Neurology 2014; 83(16): 1424–1431. [PubMed: 25217057]
16. Liu P, Liu G, Pinho MC et al. Cerebrovascular reactivity mapping using resting-state BOLD functional MRI in healthy adults and patients with Moyamoya disease. Radiology 2021; 299(2): 419–425. [PubMed: 33687287]
17. Afzali-Hashemi L, Baas KPA, Schrantee A et al. Impairment of cerebrovascular hemodynamics in patients with severe and milder forms of sickle cell disease. Front Physiol 2021; 12: 645205. [PubMed: 33959037]
18. Laux BE, Raichle ME. The effect of acetazolamide on cerebral blood flow and oxygen utilization in the rhesus monkey. J Clin Invest 1978; 62(3): 585–592. [PubMed: 99455]
19. Vorstrup S, Henriksen L, Paulson OB. Effect of acetazolamide on cerebral blood flow and cerebral metabolic rate for oxygen. J Clin Invest 1984; 74(5): 1634–1639. [PubMed: 6501565]
20. Wang K, Smith ZM, Buxton RB et al. Acetazolamide during acute hypoxia improves tissue oxygenation in the human brain. J Appl Physiol 2015; 119(12): 1494–1500. [PubMed: 26472861]
21. Berson FG, Epstein DL, Grant WM et al. Acetazolamide dosage forms in the treatment of glaucoma. Arch Ophthalmol 1980; 98(6): 1051–1054. [PubMed: 6770801]
22. Ansell B, Clarke E. Acetazolamide in treatment of epilepsy. Br Med J 1956; 1(4968): 650–654. [PubMed: 20788515]
23. Ritchie ND, Baggott AV, Andrew Todd WT. Acetazolamide for the prevention of acute mountain sickness--a systematic review and meta-analysis. J Travel Med 2012; 19(5): 298–307. [PubMed: 22943270]

24. So Y, Lee HY, Kim SK et al. Prediction of the clinical outcome of pediatric moyamoya disease with postoperative basal/acetazolamide stress brain perfusion SPECT after revascularization surgery. Stroke 2005; 36(7): 1485–1489. [PubMed: 15947261]
25. Lee M, Zaharchuk G, Guzman R et al. Quantitative hemodynamic studies in moyamoya disease: a review. Neurosurg Focus 2009; 26(4): E5.
26. Nikolin B, Imamovic B, Medanhodzic-Vuk S et al. High perfomance liquid chromatography in pharmaceutical analyses. Bosn J Basic Med Sci 2004; 4(2): 5–9.
27. Lotz J, Meier C, Leppert A et al. Cardiovascular flow measurement with phase-contrast MR imaging: Basic facts and implementation. RadioGraphics 2002; 22: 651–671. [PubMed: 12006694]
28. Alsop DC, Detre JA, Golay X et al. Recommended implementation of arterial spin-labeled perfusion MRI for clinical applications: A consensus of the ISMRM perfusion study group and the European consortium for ASL in dementia. Magn Reson Med 2015; 73(1): 102–116. [PubMed: 24715426]
29. Golde WT, Gollobin P, Rodriguez LL. A rapid, simple, and humane method for submandibular bleeding of mice using a lancet. Lab Anim (NY) 2005; 34(9): 39–43.
30. Wei Z, Chen L, Hou X et al. Age-related alterations in brain perfusion, venous oxygenation, and oxygen metabolic rate of mice: A 17-month longitudinal MRI study. Front Neurol 2020; 11: 559. [PubMed: 32595596]
31. Bruder N, Cohen B, Pellissier D et al. The effect of hemodilution on cerebral blood flow velocity in anesthetized patients. Anesth Analg 1998; 86(2): 320–324. [PubMed: 9459242]
32. Wei Z, Chen L, Lin Z et al. Optimization of phase-contrast MRI for the estimation of global cerebral blood flow of mice at 11.7T. Magn Reson Med 2019; 81(4): 2566–2575. [PubMed: 30393888]
33. Wei Z, Xu J, Chen L et al. Brain metabolism in tau and amyloid mouse models of Alzheimer's disease: An MRI study. NMR Biomed 2021; e4568. [PubMed: 34050996]
34. Hirschler L, Debacker CS, Voiron J et al. Interpulse phase corrections for unbalanced pseudo-continuous arterial spin labeling at high magnetic field. Magn Reson Med 2018; 79(3): 1314–1324. [PubMed: 28585234]
35. Hirschler L, Munting LP, Khmelinskii A et al. Transit time mapping in the mouse brain using time-encoded pCASL. NMR Biomed 2018; 31: e3855.
36. Meyer CE, Kurth F, Lepore S et al. In vivo magnetic resonance images reveal neuroanatomical sex differences through the application of voxel-based morphometry in C57BL/6 mice. Neuroimage 2017; 163: 197–205. [PubMed: 28923275]
37. Wells JA, Holmes HE, O'Callaghan JM et al. Increased cerebral vascular reactivity in the tau expressing rTg4510 mouse: evidence against the role of tau pathology to impair vascular health in Alzheimer's disease. J Cereb Blood Flow Metab 2015; 35(3): 359–362. [PubMed: 25515210]
38. Chandra SB, Mohan S, Ford BM et al. Targeted overexpression of endothelial nitric oxide synthase in endothelial cells improves cerebrovascular reactivity in Ins2Akita-type-1 diabetic mice. J Cereb Blood Flow Metab 2016; 36(6): 1135–1142. [PubMed: 26661212]
39. Brothers RO, Atlas N, Cowdrick KR et al. Cerebrovascular reactivity measured in awake mice using diffuse correlation spectroscopy. Neurophotonics 2021; 8(1): 015007. [PubMed: 33665230]
40. Munting LP, Derieppe M, Suidgeest E et al. Cerebral blood flow and cerebrovascular reactivity are preserved in a mouse model of cerebral microvascular amyloidosis. Elife 2021; 10: e61279. [PubMed: 33577447]
41. Lynch CE, Eisenbaum M, Algamal M et al. Impairment of cerebrovascular reactivity in response to hypercapnic challenge in a mouse model of repetitive mild traumatic brain injury. J Cereb Blood Flow Metab 2021; 41(6): 1362–1378. [PubMed: 33050825]
42. Wenzel J, Hansen CE, Bettoni C et al. Impaired endothelium-mediated cerebrovascular reactivity promotes anxiety and respiration disorders in mice. Proc Natl Acad Sci U S A 2020; 117(3): 1753–1761. [PubMed: 31896584]
43. Govaerts K, Lechat B, Struys T et al. Longitudinal assessment of cerebral perfusion and vascular response to hypoventilation in a bigenic mouse model of Alzheimer's disease with amyloid and tau pathology. NMR Biomed 2019; 32(2): e4037. [PubMed: 30489666]

44. Wolthuis EK, Vlaar AP, Choi G et al. Mechanical ventilation using non-injurious ventilation settings causes lung injury in the absence of pre-existing lung injury in healthy mice. Crit Care 2009; 13(1): R1. [PubMed: 19152704]
45. Munting LP, Derieppe MPP, Suidgeest E et al. Influence of different isoflurane anesthesia protocols on murine cerebral hemodynamics measured with pseudo-continuous arterial spin labeling. NMR Biomed 2019; 32(8): e4105. [PubMed: 31172591]
46. Stout RW, Cho D, Gaunt SD et al. Transcutaneous blood gas monitoring in the rat. Comparative Med 2001; 51(6): 524–533.
47. ten Hove MW, Friedman DI, Patel AD et al. Safety and tolerability of acetazolamide in the idiopathic intracranial hypertension treatment trial. J Neuroophthalmol 2016; 36(1): 13–19. [PubMed: 26587993]
48. Ritschel WA, Paulos C, Arancibia A et al. Pharmacokinetics of acetazolamide in healthy volunteers after short- and long-term exposure to high altitude. J Clin Pharmacol 1998; 38(6): 533–9. [PubMed: 9650543]
49. Reagan-Shaw S, Nihal M, Ahmad N. Dose translation from animal to human studies revisited. FASEB J 2008; 22(3): 659–661. [PubMed: 17942826]
50. Scotton WJ, Botfield HF, Westgate CS et al. Topiramate is more effective than acetazolamide at lowering intracranial pressure. Cephalalgia 2019; 39(2): 209–218. [PubMed: 29898611]
51. Matthews E, Hanna MG. Muscle channelopathies: does the predicted channel gating pore offer new treatment insights for hypokalaemic periodic paralysis? J Physiol 2010; 588(Pt 11): 1879–1886. [PubMed: 20123788]
52. Lu H, Xu F, Rodrigue KM et al. Alterations in cerebral metabolic rate and blood supply across the adult lifespan. Cereb Cortex 2011; 21(6): 1426–1634. [PubMed: 21051551]
53. Chen JJ, Rosas HD, Salat DH. Age-associated reductions in cerebral blood flow are independent from regional atrophy. Neuroimage 2011; 55(2): 468–478. [PubMed: 21167947]
54. Xu J, Qin Q, Wu D et al. Steady pulsed imaging and labeling scheme for noninvasive perfusion imaging. Magn Reson Med 2016; 75(1): 238–48. [PubMed: 25732958]
55. Braun DJ, Abner E, Bakshi V et al. Blood Flow Deficits and Cerebrovascular Changes in a Dietary Model of Hyperhomocysteinemia. ASN Neuro 2019; 11: 1759091419865788.
56. Bohn KA, Adkins CE, Mittapalli RK et al. Semi-automated rapid quantification of brain vessel density utilizing fluorescent microscopy. J Neurosci Methods 2016; 270: 124–131. [PubMed: 27321229]
57. Liu H, Zhang C, Xu J et al. Huntingtin silencing delays onset and slows progression of Huntington's disease: A biomarker study. Brain 2021; 144(10): 3101–3113. [PubMed: 34043007]
58. Sudduth TL, Weekman EM, Price BR et al. Time-course of glial changes in the hyperhomocysteinemia model of vascular cognitive impairment and dementia (VCID). Neuroscience 2017; 341: 42–51. [PubMed: 27890830]

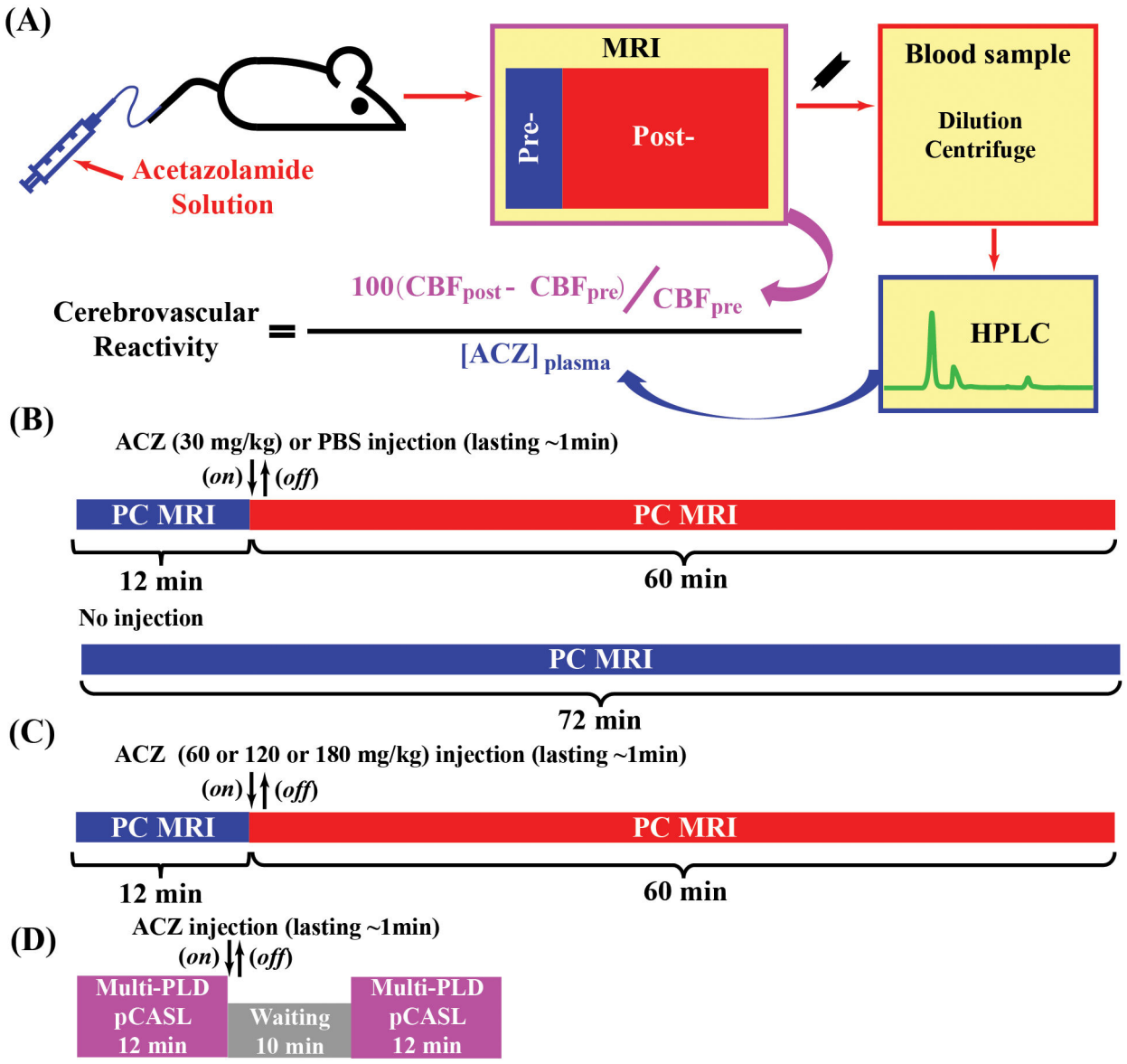

Figure 1.

Schematic diagrams of cerebrovascular reactivity (CVR) MRI using ACZ challenge. (A) procedures of ACZ-based mouse CVR experiments: animal preparation; pre- and post-injection MRI scans, blood preparation, high-performance liquid chromatography (HPLC) analysis of blood samples to determine plasma ACZ level, and final calculation of CVR. (B, C, and D) timelines for Study 1, Study 2 and Study 3, respectively. Regarding (B) and (C), an MRI session consisted of 30 PC scans (5 as baseline [12 min] and 25 as post-injection [60 min]). The injection took place at the beginning of 6th scan and lasted for about 1min. No-injection experiments also had 30 PC scans.

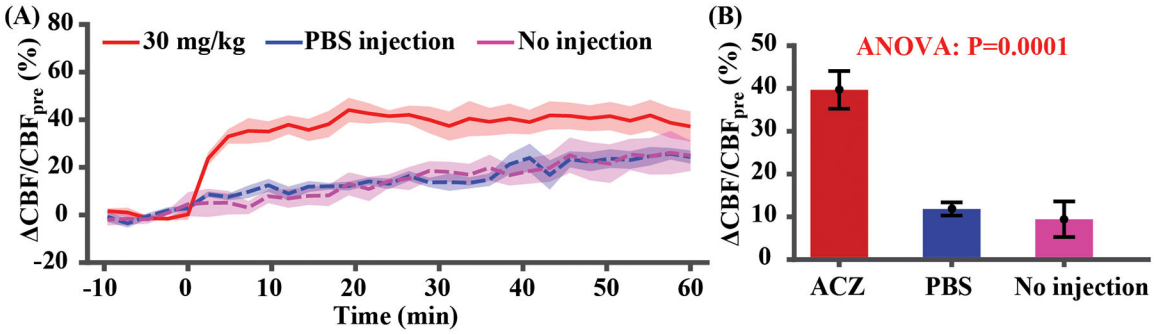

Figure 2.

CBF responses to 30 mg/kg ACZ challenge, PBS injection, and no injection (N=5). (A) Time-course of CBF changes. Time 0 indicates the start of injection. (B) Quantitative CBF changes based on the average of data during 10–20 minutes post-injection. Error bar denotes the standard error across mice.

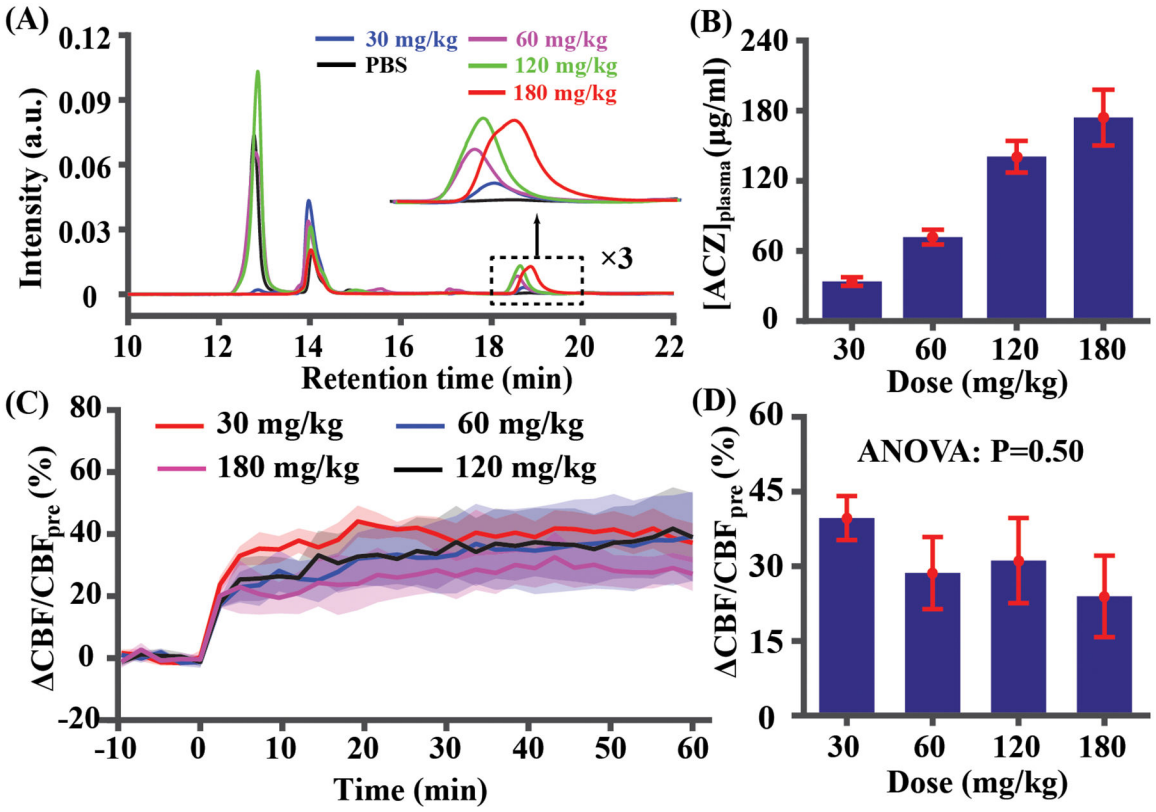

Figure 3.

$[ACZ]_{plasma}$ and vascular responses of different doses (30, 60, 120, and 180 mg/kg) (N=5). (A) HPLC chromatograms in a representative mouse. (B) Quantitative concentration values at different doses. (C) Time-courses of vascular responses at different doses. Time 0 indicates the start of injection. (D) Quantitative CBF changes based on the average of data during 10–20 minutes post-injection. Error bar denotes the standard error across mice.

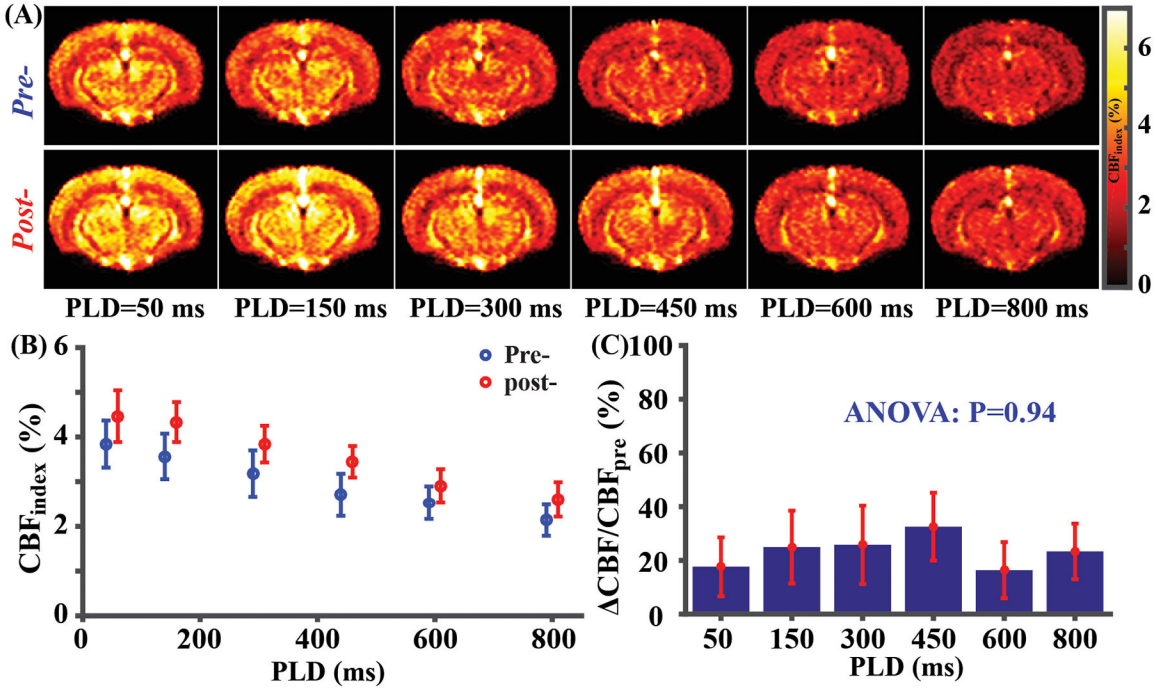

Figure 4.

CVR mapping results (N=4) with multi-PLD pCASL. (A) Average pre- and post-injection CBF weighted images at different PLDs. (B) Whole-brain CBF weighted signal for pre- and post-injection state at different PLDs. A small horizontal displacement between pre- (blue) and post-data (red) was added for display purposes. (C) Whole-brain CBF change ($\Delta CBF/CBF_{pre}$) at different PLDs. Error bars denote standard errors across mice.

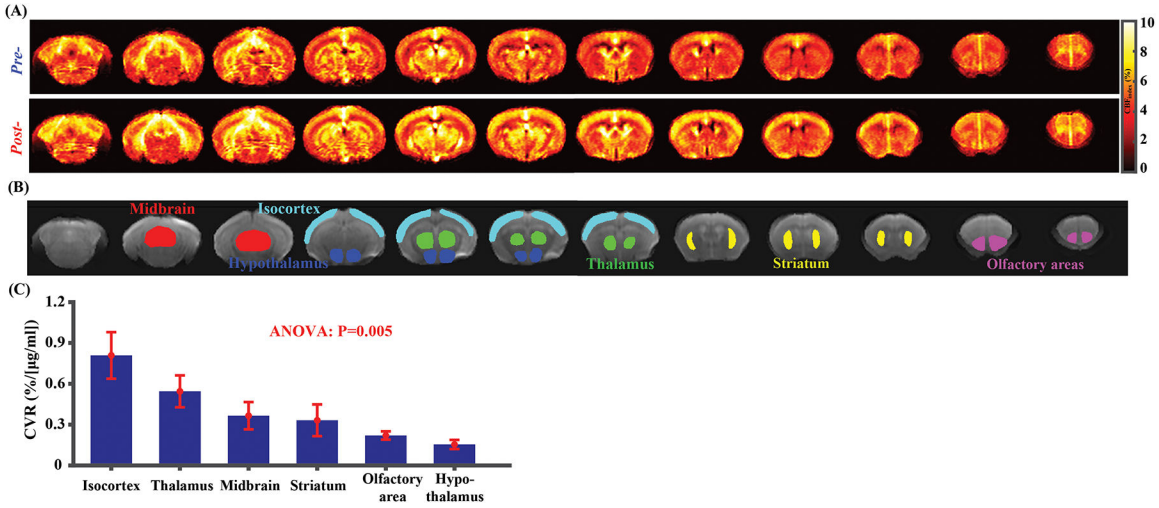

Figure 5.

CVR mapping results (N=4) with single-PLD pCASL. (A) represents average CBF_{index} images at pre- and post-injection conditions for difference slices. (B) ROI overlaid on the averaged pCASL control images. (C) CVR comparisons among different brain regions. Error bars denote standard errors across mice.